

See discussions, stats, and author profiles for this publication at: <https://www.researchgate.net/publication/249994424>

# Dynamic Optical Nonlinearities in Aniline Tetramers

ARTICLE *in* THE JOURNAL OF PHYSICAL CHEMISTRY B · DECEMBER 2004

Impact Factor: 3.3 · DOI: 10.1021/jp0495444

CITATIONS

11

READS

27

5 AUTHORS, INCLUDING:



**Paulo Franzen**

Universidade Federal do Rio Grande do Sul

15 PUBLICATIONS 66 CITATIONS

SEE PROFILE



**Leonardo De Boni**

University of São Paulo

103 PUBLICATIONS 1,140 CITATIONS

SEE PROFILE



**Cleber R Mendonca**

University of São Paulo

245 PUBLICATIONS 2,428 CITATIONS

SEE PROFILE

## Dynamic Optical Nonlinearities in Aniline Tetramers

P. L. Franzen, L. De Boni, D. S. Santos, Jr., C. R. Mendonça, and S. C. Zílio\*

*Instituto de Física de São Carlos, Universidade de São Paulo, Caixa Postal 369, 13560-970 São Carlos, SP, Brazil**Received: February 2, 2004; In Final Form: September 30, 2004*

Nonlinear optical properties of phenyl/ $\text{NH}_2$  end-capped tetraaniline in dimethyl sulfoxide solutions were investigated as a function of the tetraaniline concentration for both doped and undoped samples. We employed the single beam Z-scan technique with 70-ps-duration pulses at 532 nm, in association with others complementary techniques such as UV–vis absorption spectroscopy and time-resolved fluorescence. Our results show that both the nonlinear refractive index and the nonlinear absorption diminish for the doped sample, following the same behavior of the absorption coefficient.

## Introduction

Conductive  $\pi$ -conjugated polymers are promising materials for technological applications.<sup>1,2</sup> In particular, polyaniline (PAni) has been extensively investigated because of its high electric conductivity, excellent environmental stability, and ease of preparation. It possesses a nitrogen atom between phenyl rings, which allows the existence of different oxidation states (doping) that can affect its physical properties. In its undoped (nonconducting) state, PAni can exist as three different bases: emeraldine, leucoemeraldine, and pernigraniline.<sup>3,4</sup> The doping process, achieved through the addition of an acid, associates protons to nitrogen atoms and results in a displacement of  $\pi$  electrons.<sup>5,6</sup> These electrons are responsible for the high optical nonlinearities observed in organic materials because the relatively weak  $\pi$ -binding allows the necessary electronic mobility for the nonlinear response.<sup>7</sup>

Although optical nonlinearities have already been studied in PAni,<sup>8–10</sup> it seems worthwhile to investigate its corresponding oligomers because the physical and chemical properties of macromolecular materials in the polymeric form are usually more difficult to analyze. They generally have a considerable size dispersion that makes it difficult, if not impossible, to associate these properties to the polymer's backbone length. For polyanilines, MacDiarmid et al.<sup>11</sup> recently observed geometrical (cis and trans) and positional isomers of phenyl/ $\text{NH}_2$  end-capped tetraaniline. The existence of such geometrical isomers allowed the observation of dichroism of aniline tetramers in polymeric films.<sup>12</sup>

The present work investigates the nonlinear optical properties of phenyl/ $\text{NH}_2$  end-capped tetraaniline shown in the inset of Figure 1, with the purpose of achieving a better insight on the optical nonlinearities of polyanilines, although these have a much higher polymerization degree and size dispersion than tetraaniline. In particular, we seek to find out how the doping process affects the nonlinear properties and to compare the magnitude of the nonlinearities of molecules with very different sizes and conjugation lengths.

## Experimental Section

The samples studied were solutions of phenyl/ $\text{NH}_2$  end-capped tetraaniline base (emeraldine oxidation state) dissolved

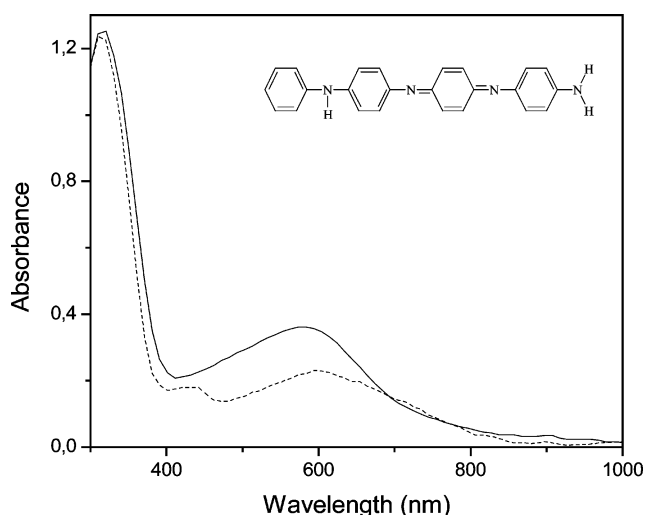


**Figure 1.** Absorbance spectra ( $-\log(I/I_0)$ ) of sample 3. The solid line refers to the undoped sample, while the dashed line corresponds to the fully doped sample. The inset shows the structural form of the phenyl/ $\text{NH}_2$  end-capped aniline tetramer molecule.

in  $\text{C}_2\text{H}_6\text{Os}$  (dimethyl sulfoxide, dubbed as DMSO) and magnetically stirred overnight. The aniline tetramer was synthesized according to the procedure described in ref 12. With the aim of verifying the existence of any aggregation process, we prepared four solutions by the addition of different amounts of DMSO. Their concentrations, in units of  $10^{17} \text{ cm}^{-3}$ , are as follows: sample 1, 0.09; sample 2, 0.72; sample 3, 1.28; and sample 4, 3.16. However, most of the experiments were carried out in sample 3, either in its undoped form or by fully doping it by the addition of hydrochloric acid at 0.2 mol/L.

Absorption and fluorescence spectra were measured aiming at obtaining parameters that are necessary for the calculations of excited-state cross-sections and relaxation times. All optical measurements, including those with the Z-scan technique, were carried out at room temperature with the sample placed in a 2 mm-long quartz cuvette. The UV–vis absorption spectra between 300 and 1100 nm were measured with a Cary-17 spectrophotometer. By determining the absorbance,  $A$ , and the concentration,  $N$ , the ground-state absorption cross-section,  $\sigma_g$ , can be evaluated through the relation  $\alpha_g = 2.3A/L = N\sigma_g$ , where  $\alpha_g$  is the ground-state absorption coefficient.

\* Corresponding author. E-mail: zilio@ifsc.usp.br.

The fluorescence spectra were measured with a USB 2000 ocean optics spectrometer, using pulsed excitation at 351 and 520 nm from an optical parametric amplifier pumped by a commercial chirped pulse amplified (CPA) laser operating at 775 nm, with a 1 kHz repetition rate. The time-resolved fluorescence evolution was obtained by exciting the sample with single 70 ps-duration pulses at 532 nm, with the same laser used in Z-scan measurements described below. Because the strongest fluorescence spectral features for pumping at this wavelength are above 600 nm, a high-pass filter ( $\lambda > 590$  nm) was placed in front of a fast detector (rise time: 1 ns) plugged into a 1 GHz digital oscilloscope connected to a personal computer.

Optical nonlinearities were determined with the single beam Z-scan technique.<sup>13</sup> The pump source was a frequency-doubled, 70 ps *Q*-switched and mode-locked Nd:YAG laser operating at 532 nm. A single pulse was extracted from the *Q*-switch envelope by means of a Pockels cell whose voltage level was used to control the energy delivered to the experiment. We employed a 5 Hz repetition rate, which is low enough to avoid residual thermal contributions from consecutive pulses produced by the laser. The beam was focused onto the quartz cuvette with a lens of focal length  $f = 12$  cm, resulting in a diameter of 40  $\mu\text{m}$  at the focal plane. As is usually done in Z-scan measurements, the transmittance through a small aperture placed at the far field position is used to determine the nonlinear refraction, while the nonlinear absorption measures all light coming from the sample, in an open aperture configuration.<sup>13</sup> These signals are measured by fast detectors (rise time: 1 ns), averaged in a 1 GHz digital oscilloscope and fed into a homemade data acquisition system based on a personal computer (PC). Because our detection system has a rise time much slower than the 70 ps pulse duration, each peak height measured is proportional to the corresponding pulse fluence.

## Results and Discussion

The UV-vis absorbance spectra shown in Figure 1 are similar to those of high molecular weight polyanilines<sup>14</sup> with the band at 315 nm, attributed to  $\pi \rightarrow \pi^*$  transitions,<sup>5</sup> appearing somewhat shifted from its usual position in polyanilines.<sup>4</sup> Different oxidation states do not change this band appreciably. On the other hand, the absorption band at 580 nm, usually attributed to the  $n \rightarrow \pi^*$  transitions,<sup>2</sup> is strongly affected by doping, as seen in Figure 1. From these measurements, we calculate the cross sections for  $n \rightarrow \pi^*$  transitions at 532 nm as  $\sigma_g = 2.9 \times 10^{-17}$  and  $1.8 \times 10^{-17} \text{ cm}^2$ , for undoped and doped samples, respectively.

The fluorescence spectra depicted in Figure 2 show a broad emission band centered at 440 nm for excitation of the  $\pi \rightarrow \pi^*$  transition at 351 nm (solid line), while excitation of the  $n \rightarrow \pi^*$  transition at 520 nm results in an emission band centered at 600 nm (dashed line). The time-resolved fluorescence measurement carried out with single 532 nm pulses is shown in Figure 3. The fluorescence lifetime corresponding to the  $n \rightarrow \pi^*$  absorption,  $\tau_f$ , was determined to be about 3.4 ns. The knowledge of  $\sigma_g$  and  $\tau_f$  is important to minimize the number of parameters used to fit the results of Z-scan experiments. Although the 580 nm absorbance band decreases for doped samples, fluorescence measurements performed do not show any significant change in the band position, nor in its lifetime for different doping states.

Figure 4 presents the results of nonlinear refractive index obtained with the Z-scan technique. Its signal was found to be positive, with values ranging from 1 to 6 ( $\times 10^{-15}$ )  $\text{cm}^2/\text{W}$  for

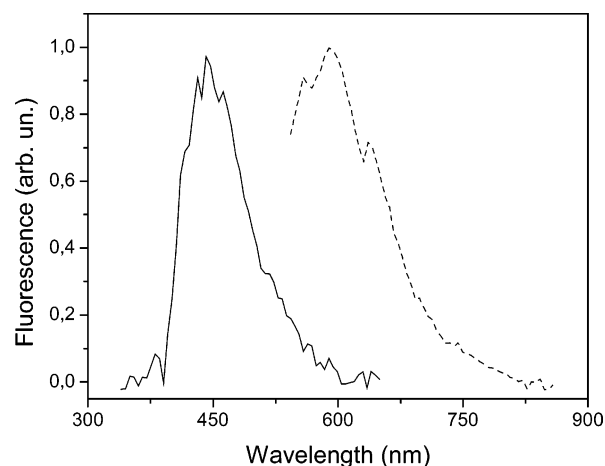


**Figure 2.** Fluorescent spectra of sample 3 for excitation at 351 nm (—) and 520 nm (---).

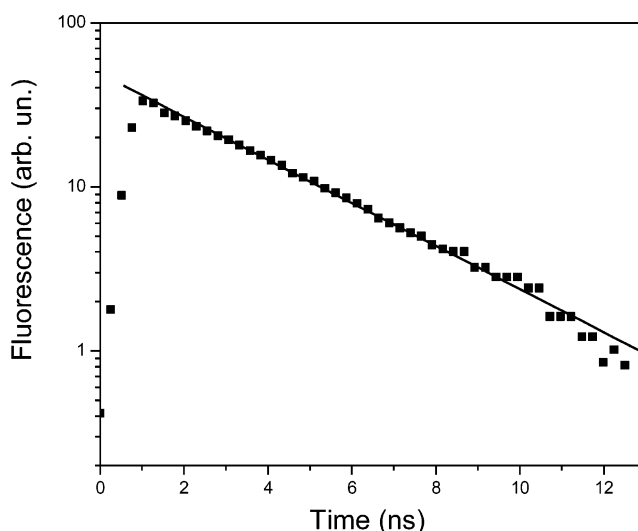


**Figure 3.** Time-resolved fluorescence measurement carried out in sample 3 with 532 nm single pulses excitation. The line corresponds to a single exponential with a decay time of 3.4 ns.

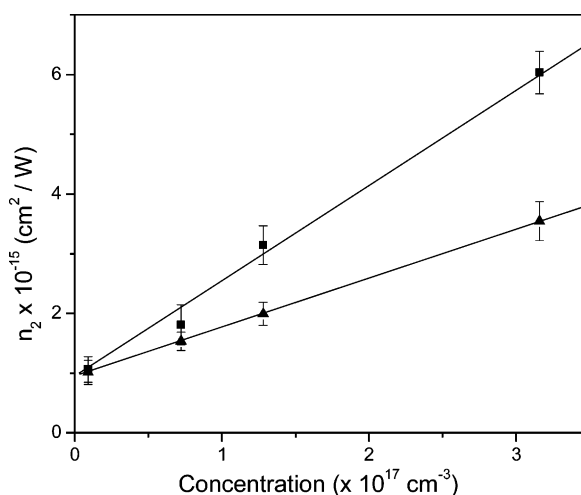


**Figure 4.** Behavior of  $n_2$  as a function of the concentration for different oxidation states. The  $\blacksquare$  symbols correspond to the undoped sample, and the  $\blacktriangle$  symbols correspond to the fully doped sample. The lines are the best linear fit for each case.

the concentrations used. Measurements carried out in polyaniline/DMSO solutions<sup>15</sup> presented results that are on the same order of magnitude as those presented here, indicating that the

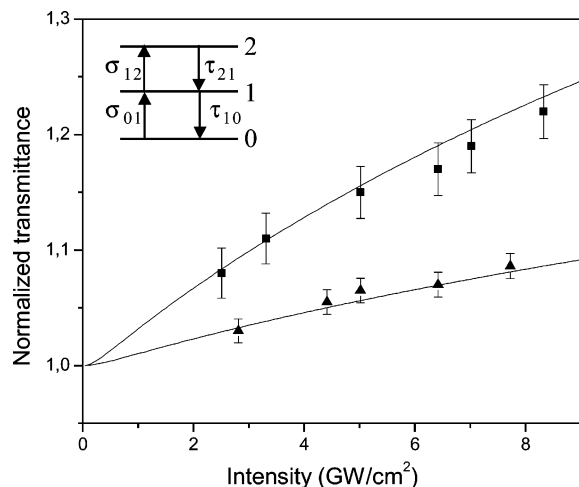


**Figure 5.** Nonlinear absorption as a function of light intensity. The ■ and ▲ symbols correspond, respectively, to undoped and doped samples. The lines are the best fit achieved with the energy-level diagram shown in the inset.

nonlinearity is not directly proportional to the polymer's chain size. The linear dependence on the concentration suggests that any aggregation process can be disregarded. As the concentration decreases, the value of  $n_2$  tends to that of pure DMSO. Moreover,  $n_2$  diminishes with the doping degree, in the same proportion of the linear absorption.

The nonlinear absorption behavior of the tetraaniline molecule is that of a saturable absorber.<sup>16</sup> As expected, the magnitude of the effect tends to diminish with the doping degree, following the cross-section behavior, as depicted in Figure 5. The normalized transmittance at the focal plane has a nearly linear dependence as a function of the light intensity for both doped and undoped samples. The saturation intensity of each sample can be estimated from its cross section and fluorescence lifetime according to  $I_s = \hbar\omega/\sigma\tau$ . We obtained 3.8 and 6.5 MW/cm<sup>2</sup> for the undoped and doped samples, respectively. These values are much lower than the intensities actually employed in our measurements. However, we hardly see any saturation in the plots of Figure 5, which is unexpected a priori, because the lifetime of the first excited state is much longer than pulse duration and the molecules cannot return to its ground state before the end of the pulse. To explain these results, we have to assume that transitions to higher energy levels have cross sections with values very close to that of the ground state. Let us consider the simple three-energy level model shown in the inset of Figure 5, with the corresponding rate equations:

$$\begin{aligned}\frac{dn_0}{dt} &= -n_0W_{01} + \frac{n_1}{\tau_{10}} \\ \frac{dn_1}{dt} &= n_0W_{01} - n_1W_{12} + \frac{n_2}{\tau_{21}} - \frac{n_1}{\tau_{10}}\end{aligned}$$

where  $n_i$  is the population fraction in level  $i$ ,  $W_{01} = \sigma_{01}I_0/\hbar\omega$ ,  $W_{12} = \sigma_{12}I_0/\hbar\omega$ , and  $n_0 + n_1 + n_2 = 1$ . These equations can be numerically solved by considering a Gaussian pulse and considering the intensity-dependent absorption coefficient as:

$$\alpha(I) = N(n_0\sigma_{01} + n_1\sigma_{12})$$

where  $N$  is the concentration. Here, we have assumed that the population buildup in level 2 can be neglected and no absorption from that level is considered. By using the known values of

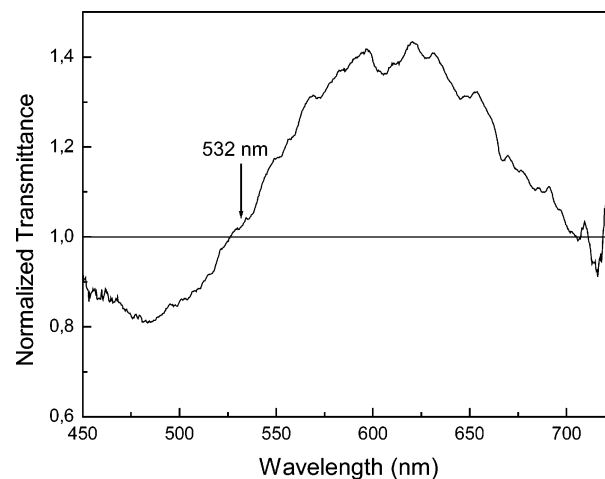


**Figure 6.** Nonlinear absorption as a function of wavelength for the undoped sample 3.

$\sigma_{01}$ ,  $\tau_{10}$ , and  $I_0$  as fixed parameters, and  $\sigma_{12}$  and  $\tau_{12}$  as the only fitting parameters, we can fit our results for  $\sigma_{12} \approx \sigma_{01}$  and  $\tau_{21}$  on the order of a few picoseconds. This fast relaxation time guarantees a negligible population in level 2. On the other hand, the similarity between the cross sections of levels 0 and 1 deserves a deeper investigation to make sure that our model has no flaw. To reach this goal, we characterized the excited-state absorption spectrum by performing open aperture Z-scan measurements as a function of wavelength with the same optical parametric amplifier used for fluorescence measurements. The result shown in Figure 6 indicates that tetraaniline behaves as a saturable absorber above 525 nm and as a reverse saturable absorber below this wavelength. In particular, the absorption cross section of the excited state ( $\sigma_{12}$ ) at 532 nm is just a few percent smaller than that of the ground state. This corroborates the validity of the three-energy-level diagram proposed.

## Conclusions

It is usually stated that  $\pi$  electrons in conjugated polymers are responsible for high optical nonlinearities in organic materials because the weak  $\pi$ -binding gives rise to the necessary electronic mobility for the nonlinear response. Although this is true for transparent media, where the excitation light is far from any resonance, our results clearly show that this does not hold for absorbers. Although we have measured just one aniline oligomer (tetraaniline) and two doping states (undoped and fully doped), it was possible to establish the importance of the electronic mobility on the optical nonlinearities. Indeed, our results demonstrated that optical nonlinearities do not depend on the electronic mobility because the addition of protons during the doping process produced a modest variation in the optical nonlinearities, which can be explained by the decrease of the absorption coefficient. Besides, the results for tetraaniline are comparable to those of the much longer polyaniline. These facts are clear evidence that optical nonlinearities in organic absorbers depend strongly on spectroscopic parameters such as absorption cross sections and lifetimes, and not on the electronic mobility and molecular size. We have also carried out measurements in dianiline with the same concentrations used for tetraaniline, but we did not observe any nonlinear effect. We also measured a 33% doped tetraaniline sample, but the conclusions were the same as presented earlier; the variation of the optical nonlinearities could be explained by the decrease of the absorption coefficient.

**Acknowledgment.** We gratefully acknowledge the support of the Fundação de Amparo à Pesquisa do Estado de São Paulo (FAPESP) and Conselho Nacional de Desenvolvimento Científico e Tecnológico (CNPq).

## References and Notes

- (1) Wang, Y. Z.; Sun, R. G.; Meghdadi, F.; Leising, G.; Swager, T. M.; Epstein, A. J. *Synth. Met.* **1999**, *102*, 889.
- (2) Epstein, A. J. In *Conjugated Polymers*; Brédas, J. L., Silbey, R., Eds.; Kluwer Academic Publishers: Dordrecht, Netherlands, 1991; p 211.
- (3) Libert, J.; Brédas, J. L.; Epstein, A. J. *Phys. Rev. B* **1995**, *51*, 5711.
- (4) Libert, J.; Cornil, J.; Dos Santos, D. A.; Brédas, J. L. *Phys. Rev. B* **1997**, *56*, 8638.
- (5) Zuo, F.; McCall, R. P.; Ginder, J. M.; Roe, M. G.; Leng, J. M.; Epstein, A. J.; Asturias, G. E.; Ermer, S. P.; Ray, A.; Macdiarmid, A. G. *Synth. Met.* **1989**, *29*, E445.
- (6) Kwon, O.; McKee, M. L. *J. Phys. Chem. B* **2000**, *104*, 1686.
- (7) Prasad, P. N.; Williams, D. J. *Introduction to Nonlinear Optical Effects in Molecules and Polymers*; Wiley: New York, 1991.
- (8) Petrov, D. V.; Gomes, A. S. L.; de Araújo, C. B.; de Souza, J. M.; de Azevedo, W. M.; de Melo, J. V.; Diniz, F. B. *Opt. Lett.* **1995**, *20*, 554.
- (9) Samoc, M.; Samoc, A.; Luther-Davies, B.; Swiatkiewicz, J.; Jin, C. Q.; White, J. W. *Opt. Lett.* **1995**, *20*, 2478.
- (10) Maciel, G. S.; Nikifor Rakov, A. G. B., Jr.; de Araújo, C. B.; Gomes, A. S. L. *J. Opt. Soc. Am. B* **2001**, *18*, 1099.
- (11) Macdiarmid, G.; Zhou, Y.; Feng, J. *Synth. Met.* **1999**, *100*, 131.
- (12) Mendonça, C. R.; Santos, D. S.; De Boni, L.; Balogh, D. T.; Oliveira, O. N.; Zilio, S. C. *Adv. Mater.* **2000**, *12*, 1126.
- (13) Sheik-Bahae, M.; Said, A. A.; Wei, T.; Hagan, D. J.; Van Stryland, E. W. *IEEE J. Quantum Electron.* **1990**, *QE-26*, 760.
- (14) Shimano, J. Y.; Macdiarmid, A. G. *Synth. Met.* **2001**, *123*, 251.
- (15) Pilla, V.; Mendonça, C. R.; Balogh, D.; Zilio, S. C. *Mol. Cryst. Liq. Cryst.* **2002**, *374*, 487.
- (16) Oliveira, L. C.; Catunda, T.; Zílio, S. C. *Jpn. Appl. Phys.* **1996**, *35*, 2649.